Magnetic-field-induced structural change of a two-dimensional colloid of glycerol droplets on a nematic liquid-crystal surface

Sang-In Paek, Song-Jo Kim, and Jong-Hyun Kim
Physics, Chungnam National University, 220 Gung-dong, Yuseong-gu, Daejeon 305-764, Korea
(Received 19 August 2012; published 5 March 2013)

The structural changes of a two-dimensional colloidal crystal, consisting of glycerol droplets on a nematic liquid-crystal surface, due to a magnetic field applied parallel to the liquid-crystal surface, were observed and analyzed. The hexagonal lattice arrangement of glycerol droplets transformed into a smaller, anisotropic hexagonal-like lattice when the magnetic field was applied. The intermediate stage of the transition is influenced by the way in which the magnetic field is applied. When a sufficiently strong magnetic field is applied directly, the transition proceeds by passing through a random arrangement and then through a chainlike arrangement. With a gradually increasing magnetic field, the transition starts locally and extends throughout the entire region. The relaxation processes that occur once the field is switched off are very similar, irrespective of the manner in which the field is switched off. The relaxation begins at the outside and then extends to the central regions. No tendency to form a chainlike arrangement was observed during the relaxation process. The processes during switching on and off demonstrate a hysteresis with respect to the magnetic field strength.

DOI: 10.1103/PhysRevE.87.032502 PACS number(s): 61.30.Gd, 61.30.Eb, 82.70.Dd

I. INTRODUCTION

Nematic liquid crystal (LC) has orientational order and induces electric, magnetic, and optical anisotropy in spite of its fluid nature. When small particles enter the LC, the orientational anisotropy of the LC mediates the interaction between the particles. This stimulates the formation of structures different from those found in the isotropic liquid [1–5]. The structures vary with the type of orientation of the LCs and the alignment of LCs on the particle surface.

On the surface of a relatively thick LC layer, glycerol droplets of micrometer size form two-dimensional hexagonal crystal structures [6]. This crystal structure is determined by the deformation energy of the LC. There exists an attractive force due to the coupling of the elasticity and capillary force [7–9]. There is also a repulsion originating from the elastic deformation. The distance between droplets in equilibrium increases and is proportional to the size of the droplet according to a power law with an exponent of $2/3$. For a thin LC film, the tilted LC alignment induces a chainlike arrangement of glycerol droplets.

This structure has been shown to transform from a hexagonal lattice to a chainlike structure due to the application of a horizontal magnetic field [10]. The increased dipolelike anisotropy with the magnetic field causes the linear chain arrangement. The distance between droplets was expected to decrease with the square of the magnetic field strength. The structure becomes random with increased temperature [9]. As the temperature increases, a two-dimensional phase transition occurs, and this transition can be described qualitatively by the Kosterlitz-Thouless-Halperin-Nelson-Young (KTHNY) theory [11–17]. In other words, the hexagonal structure of quasi-long-range positional order and long-range bond-orientational order melts and a short-range positional and bond-orientational order is established. During the process the structure passes through a hexatic phase characterized by a short-range positional and quasi-long-range bond-orientational order.

With increasing glycerol droplet density, the hexagonal lattice has been shown to transform irreversibly into a dense lattice [8]. The dense lattice was expected to be an isotropic hexagonal lattice, but instead had lattice constants with anisotropy of approximately 10%. The hexagonal structure was recovered by applying a vertical electric field to the LC surface. Moreover, the structure of silica beads on top of a LC is also dependent on the thickness of the LC layer and the bead density [18]. For thick LC layers, the liquid, crystal, and amorphous condensed states are passed through as the bead density is increased. With a thin LC layer, the beads align in a chainlike arrangement. Systems to which photoreactive azo dye was added indicated a light sensitive variation in the distance between glycerol droplets [19–21]. This reaction, which transforms the azo dye from trans to cis isomers, reduces the surface tension of the LC, and the distance between glycerol droplets decreases. This may be a useful tool for controlling photonic crystals with light.

In this study we used a colloidal system consisting of LC and glycerol droplets and observed the transition caused by an applied magnetic field. We examined the transition in detail and over a wide parameter range compared it to previously reported studies [10,22]. With a sufficiently strong magnetic field, the hexagonal lattice (HL) was broken and a chainlike alignment (CLA) occurred for a short time. Finally, the glycerol droplets aggregated into a hexagonal-like lattice (HLL) with small separations between droplets. We have attempted to explain these transition processes using well-known tools such as the pair-correlation function, orientational correlation function, and the bond-orientational order parameter. Moreover, to analyze the specific character of our system, we have introduced the anisotropy parameter.

II. EXPERIMENTS AND CALCULATIONS

In the experiment, 4-cyano-4′-pentylbiphenyl (5CB, from Sigma Aldrich) was used as the LC. It is nematic phase at room temperature and becomes isotropic above 36 °C.

A glycerol layer several millimeters thick was prepared in a petri dish, and an LC layer of over 100 μm thickness was added

onto the glycerol. The system was heated to approximately 40 °C and quickly cooled down, after which it was left standing for several days. Some glycerol dissolved into the LC. Although the glycerol density was higher than that of 5CB, the droplets remained on the LC surface due to the surface tension. We obtained an HL of glycerol droplets that consisted of about 400 droplets on the LC. The glycerol droplets had diameters of around 20 μm, and the glycerol droplet aggregates were limited to only within a region of diameter 1 mm, unlike in the case of typical glycerol colloidal systems. The petri dish was placed in an electromagnet, and the magnetic field applied parallel to the LC surface was up to several hundred gauss. A reflective optical microscope system was used to observe changes in the colloidal structure with and without the magnetic field. The images were obtained with a CCD camera of 2048×1536 pixels and each pixel covers 0.5×0.5 μm^2. The observations were carried out at room temperature.

We calculated the pair-correlation function, orientational correlation function, and bond-orientational order parameter to analyze the experimental data. The mathematical expressions that follow are reproduced from Ref. [14]. The pair-correlation function $g(r)$ indicates the distribution of droplets as a function of the distance between droplets and is expressed as $g(r) \equiv \langle \delta(r')\delta(r'-r)\rangle$, where $\delta(r)$ is the δ function. The brackets indicate averaging over all angles and all of the different droplets. This has a large value when the system is regularly arranged, and approaches a value of 1 for irregular structures. Therefore, it is a measure of the translational ordering of a system.

The orientational correlation function indicates the angular distribution as a function of the distance and is expressed as

$$g_{\mathrm{B}}(r) \equiv \frac{\langle \varphi_6^*(r')\varphi_6(r'-r)\rangle}{\langle \delta(r')\delta(r'-r)\rangle}.$$

The local bond orientational order parameter $\varphi_6(r)$ of hexagonal systems is expressed as

$$\varphi_6(r_m) \equiv \frac{1}{N_{\mathrm{bond}}} \sum_{n=1}^{N_{\mathrm{bond}}} \exp(6i\theta_{mn}).$$

The index n extends over the mth particle's nearest neighbors. θ_{mn} is the angle between some fixed axis and the bond joining the mth droplet with the nth droplet. N_{bond} denotes the number of m-n bonds. The orientational correlation function indicates the orientational ordering in a two-dimensional hexagonal system. The bond-orientational order parameter (Φ_6) is a measure of the structural order of a two-dimensional hexagonal system and is expressed as

$$\Phi_6 \equiv \left\langle \frac{1}{N} \sum_{m=1}^{N} \frac{1}{N_{\mathrm{bond}}} \sum_{n=1}^{N_{\mathrm{bond}}} \exp(6i\theta_{mn}) \right\rangle.$$

Here N is the number of particles. The bond-orientational order parameter is close to 1 for hexagonal ordering and much less than one for disordered structures.

In addition to the above physical quantities, we introduced the anisotropy parameter (Φ_2). During the experiment we observed the transition from an HL to a CLA along the direction of the applied magnetic field. Φ_6 is suitable for measuring the HL, but does not sufficiently represent the CLA and the transition process. We therefore introduced a new parameter, expressed as

$$\Phi_2 \equiv \left\langle \frac{1}{N} \sum_{m=1}^{N} \frac{1}{2} \sum_{n=1}^{2} \frac{1}{2} [3(\cos\theta'_{mn})^2 - 1] \right\rangle.$$

The variable n serves as an index for the two droplets nearest the mth droplet. θ'_{mn} is the angle between the line joining the mth and nth droplets and the magnetic field. The anisotropy parameter is 1 for an ideal chain arrangement. The hexagonal lattice will indicate close to zero value in anisotropic parameter due to the equivalent distribution along three orientations. The random lattices will also show near zero value for the homogeneously distributed orientations. The anisotropy parameter is expected to approach 1 for the CLA and to be small in both fluidlike alignment and in HLs.

During our calculations, the number of droplets and the size of the droplet aggregates were limited. The outer boundary should be examined, especially in the calculation of $g(r)$ and $g_{\mathrm{B}}(r)$. The ratio of the effective angle to a full circle at a given distance was corrected in the calculation of the above two functions. Then the error range of the amplitude for the nearest droplets is about 10%. It is increased about 30% for the 120 μm distance. However, the trends of the graphs indicate that the distant range is not an issue in determining the behavior. However, in the calculation of Φ_6 and Φ_2, we removed the outermost droplets from the calculation. In the calculation of Φ_6 and Φ_2, the N_{bond} droplets or the two droplets nearest a given droplet were calculated. If the distances were very different from one another, the largest value was disregarded. In this calculation, we limited the distance to 1.2 times the selected value to account for variations in droplet size. The center of the droplet was used to represent the droplet position. There was ± 1.5 μm error in the calculation of $g(r)$ and $g_{\mathrm{B}}(r)$ for the discrete position and limited number in droplets.

III. RESULTS

A. Sudden switch on and switch off of the magnetic field

A magnetic field (440 G) was applied directly and the change in the colloidal structure was observed, as shown in Fig. 1. The glycerol droplets formed a rather well-ordered HL [Fig. 1(a)] before the magnetic field was applied. The actual structure was slightly larger than shown in the image. Soon after applying the magnetic field, the HL melted into a random distribution and started to show CLA [Figs. 1(b) and 1(c)]. CLA means there is an anisotropic alignment with shorter distances along the magnetic field rather than perpendicular to the magnetic field. Over time, the structure collapsed and seemed to form an HLL with shorter distances compared to the structure shown in Fig. 1(a) [see Fig. 1(d)].

The average diameter of the glycerol droplets was 18.3 ± 1.4 μm and the average distance between neighboring droplets was 50.4 ± 5.9 μm, as shown in Fig. 1(a). With application of the magnetic field for a sufficient time, the average diameter of the glycerol droplets became 18.0 ± 1.4 μm, and the average distance between nearest droplets became 19.8 ± 1.7 μm. The equilibrium distance before the magnetic field was applied was rather large compared to previous results [6–8]. Typically,

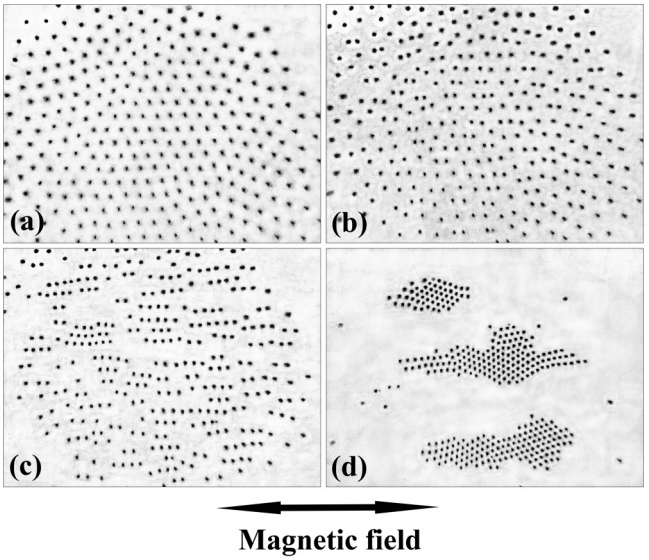

FIG. 1. Structural change with a fixed magnetic field was applied. (a) Immediately before application of the magnetic field, (b) after 3 h, (c) after 13 h, and (d) after 24 h. The three large aggregates in (d) eventually clustered together to form a lump. The width of these images is 1040 μm. The contrast and color of the images were modified for clarity.

the distance between neighboring droplets is approximately twice the diameter of the droplets. The previously published results all correspond to droplets distributed over an area that extends beyond the region of interest. However, in our case, the location of the droplets was limited to within the imaged region. The large distance may be partially due to the pressureless environment outside the HL. The magnetic field almost forced the droplets to merge because the distance between droplets was only slightly larger than the diameters of the droplets. The pressure from the other droplets was not significant enough to force a change in the droplet shape.

The change in the structure shown in Fig. 1 was analyzed using the procedure shown in Fig. 2. Figure 2(a) shows Φ_6 and Φ_2 as functions of time. Φ_6 is approximately 0.4 to begin with, which is relatively low for the following reasons. The density of droplets was smooth and dependent on the distance from the center of the image. The droplet size was not perfectly uniform, but had an irregularity of about 10%. Moreover, it may not be sufficiently completely stabilized at that state. Over time, Φ_6 decreased slightly and returned to a rather large value. On the other hand, Φ_2 started from a tiny value and increased with the development of CLA. However, with the collapse to the short distance HLL, it decreased to almost zero. In summary, starting from the HL, there was a random arrangement for a brief time before CLA developed, and finally, this transformed into HLL.

Figures 2(b) and 2(c) show $g(r)$ and $g_B(r)$ at selected times. Both graphs indicate that translational and orientational ordering was relatively high when the magnetic field was first applied. The double-peaks shape of the second peak in $g(r)$ is expected in an ideal HL. However, there is no clue of the double peaks in 0 h graph of Fig. 2(b). After the magnetic field had been applied for 6 h, the disorder increased and the

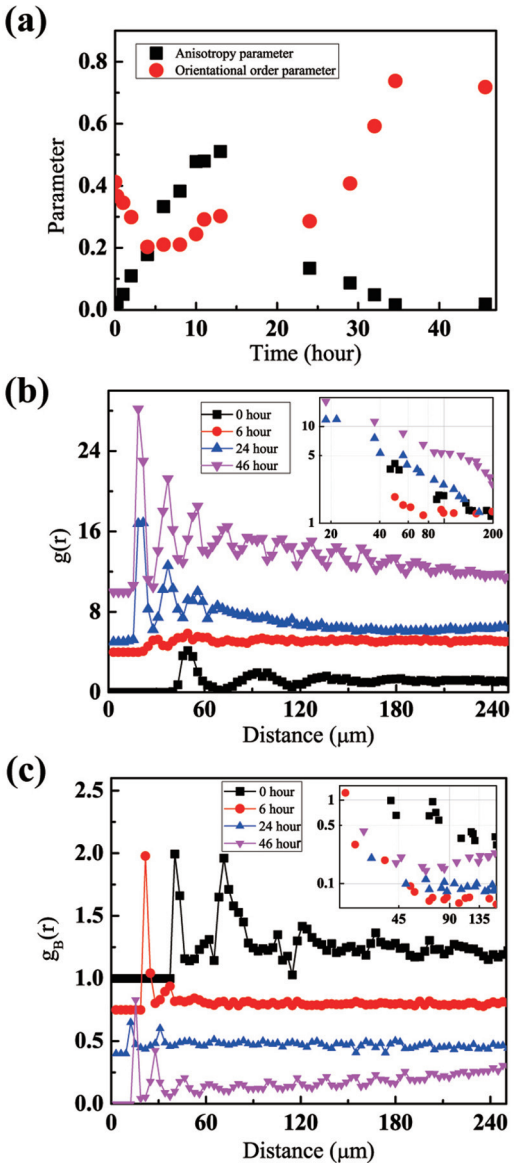

FIG. 2. (Color online) Calculation of the structural change shown in Fig. 1. (a) The anisotropy parameter and orientation order parameter as functions of time. (b) Pair-correlation function for the selected cases. (c) Orientational correlation functions for the selected cases. The small box in each figure is the log-log plot of the near peak points of $g(r)$ and $g_B(r)$ as function of distance (μm). Plots in (b) and (c) were vertically shifted to avoid the overlapping.

ordering disappeared even over short distances. For longer magnetic field application times, both functions increased with decreasing distance between droplets. The $g(r)$ curve was similar to a power law for the first 4 h, and over longer times, its behavior was similar to an exponential decay. The exponent of the power law was almost 1, much larger than the value expected from the KTHNY theory [12,13,16]. After 24 h, the power lawlike decay reappeared, and the exponent decreased to 0.7 by hour 46. $g_B(r)$ also shows a similar trend over a different time scale. For a short application time, the $g_B(r)$ curve resembled a power law, and it became like an exponential decay with increased application time. Between times of 4 and 24 h, the decay was exponential. Between hours

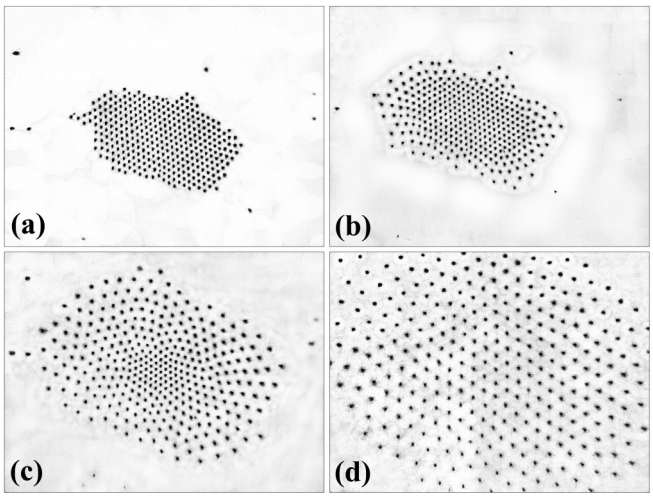

FIG. 3. Structural change when switching the magnetic field off. (a) Immediately before the magnetic field was switched off, (b) after 1 h, (c) after 7 h, and (d) after 47 h. The width of the image in (d) is 1040 μm. The contrast and color of the images were modified for clarity.

35 and 46, the relaxation followed a power law within a limited range of separation. The exponents of the power law decays were larger than the values predicted by the KTHNY theory. At hour 46, $g_B(r)$ increased with distance in the range of larger than 60 μm. This is because the convergence of the positional correlation to the value 1 occurred faster than the decrease of orientational correlation with distance.

After turning off the magnetic field, the collapsed HL returned to the arrangement that was present before the magnetic field was turned on, as shown in Fig. 3. The change occurred relatively slowly, especially at lower densities, as shown in Fig. 3(d). The recovery process was not an exact reversal of the processes that occurred when the magnetic field was applied. Here the recovering region continuously extended from the edge of the area to the inside, and CLA did not occur.

In the process illustrated in Fig. 3, Φ_2 was close to zero throughout the process, as shown in Fig. 4(a). Φ_6 decreased abruptly due to the melting and spreading of the HL and then increased. The behavior of these parameters is very different from when the magnetic field was switched on. $g(r)$ and $g_B(r)$ indicate that the structure 6 h after switching off the magnetic field had a very short correlation length. In fact, $g(r)$ exhibited power lawlike decay for the first 6 h. Subsequently, $g(r)$ decayed exponentially until about hour 40. Power lawlike decay appeared again after 40 h. The power law exponent was approximately 1. In the case of $g_B(r)$, the behavior was similar to that of $g(r)$ with the exception of an increase in value for short times. The decay was like a power law for a short time, but it became an exponential decay beginning at hour 3 and returned to a power lawlike decay after 20 h with an exponent close to 1.

B. Gradual switching on and off of the magnetic field

Figure 5 shows the structural changes that occurred when the magnetic field was increased step-by-step. The initial and

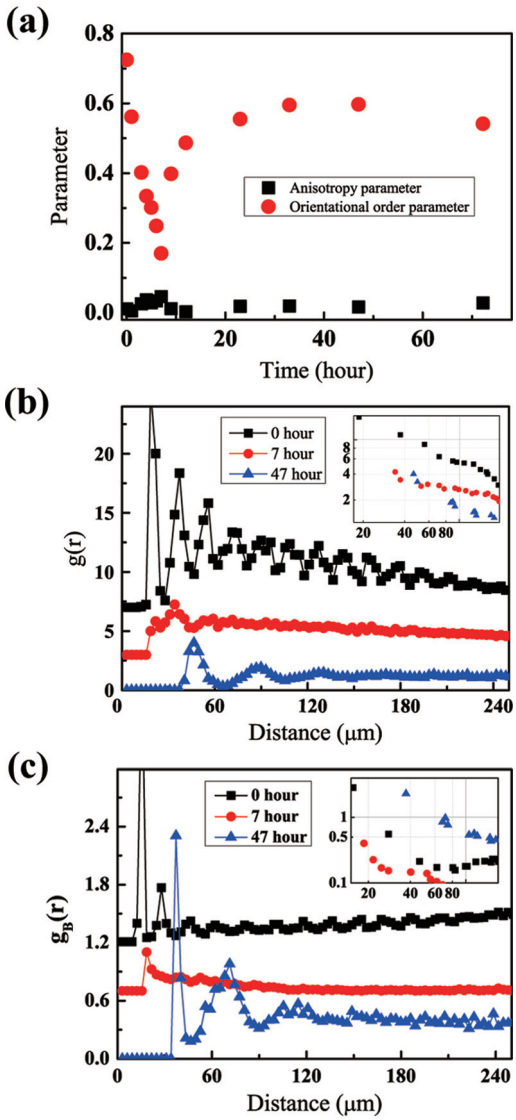

FIG. 4. (Color online) Calculation of the structural change shown in Fig. 3. (a) The anisotropy parameter and orientation order parameter as functions of time. (b) Pair-correlation function for the selected cases. (c) Orientational correlation function for the selected cases. The small box in each figure is the log-log plot of the near peak points of $g(r)$ and $g_B(r)$ as function of distance (μm). Plots in (b) and (c) were vertically shifted to avoid the overlapping.

final structures were very similar to those shown in Fig. 1. However, the process proceeded in a slightly different manner. With a weak magnetic field (less than 210 G), no structural changes were observed even for long application times of more than 20 h. With a stronger magnetic field (300 G), the entire structure seemed to shrink as shown in Fig. 5(b). Figure 5(c) shows the local reduction in lattice spacing with a magnetic field of 370 G. Longer application times drove the reduction of lattice spacing throughout the system, as shown in Fig. 5(d).

The structural changes that occurred when the magnetic field was reduced step-by-step are shown in Fig. 6. When the magnetic field was reduced, the outer droplets began to disperse, and this dispersion spread to the inner droplets. This

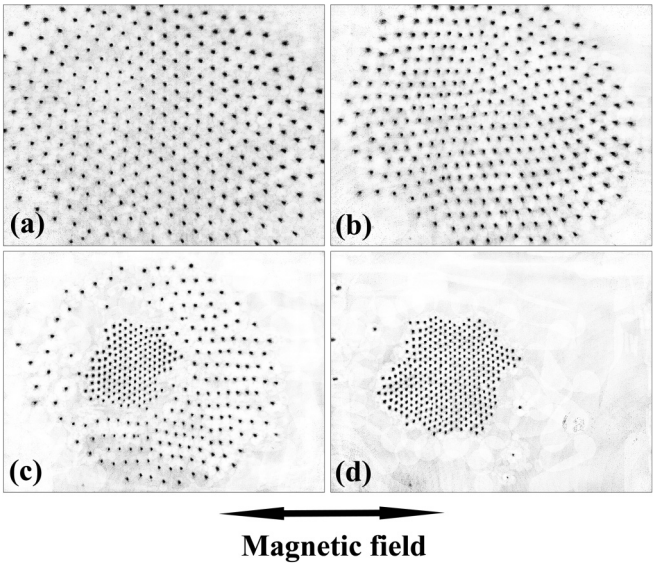

FIG. 5. Structural change when the magnetic field is increased and time elapsed. (a) Before the magnetic field was switched on, (b) after a magnetic field of 300 G was applied for 130 h, (c) after a magnetic field of 370 G was applied 13 h after (b), and (d) after a magnetic field of 370 G was applied for 60 h after (b). Before (b), a magnetic field of 210 G was applied, but no change was observed. The width of the image of (a) is 1040 μm. The contrast and color of the images were modified for clarity.

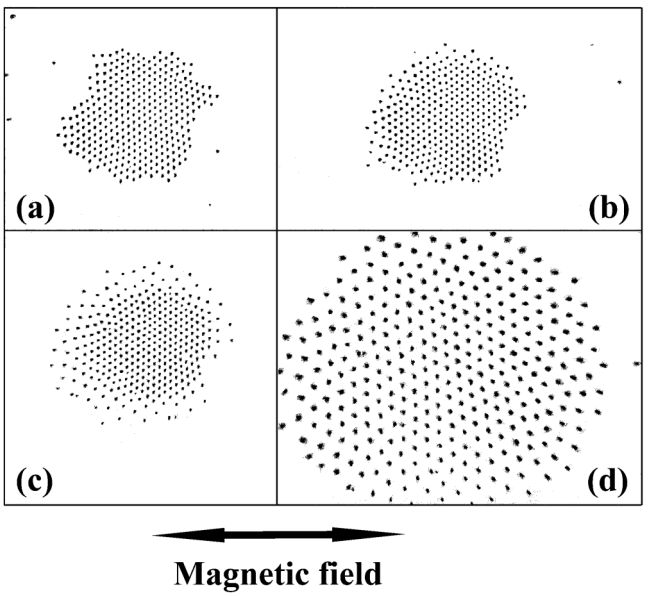

FIG. 6. Structural change when reducing the magnetic field strength step-by-step. (a) After application of a magnetic field of 370 G for sufficient time to stabilize the structure, (b) 210 G for 170 h, (c) 140 G for 3.5 h, and (d) 140 G for 60 h. A magnetic field of 300 G was applied for 73 h between (a) and (b) but no change was observed. The structure shown in (d) is not saturated, and after 90 h, it returned to a structure similar to that before the magnetic field was applied. The contrast and color of the images were modified for clarity.

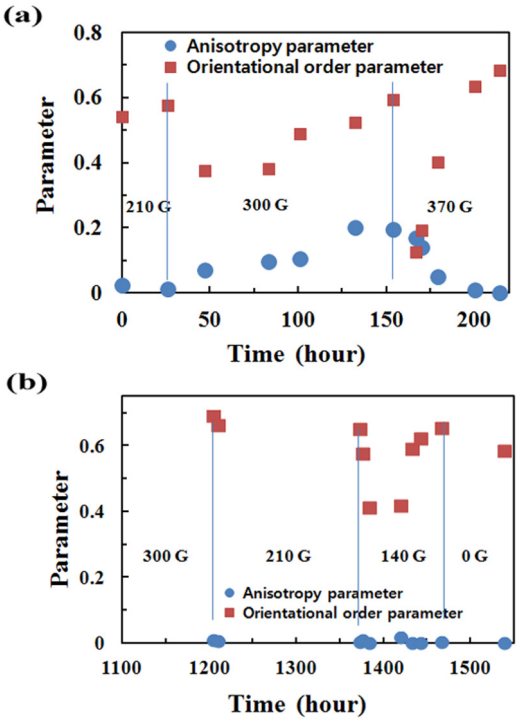

FIG. 7. (Color online) Calculation of the anisotropy parameter and orientational order parameter. The structural change is due to a step-by-step increase and decrease of the applied magnetic field strength. (a) Structural changes with increasing magnetic field. This corresponds to Fig. 5. (b) Structural changes with decreasing magnetic field. This corresponds to Fig. 6. In the case of (b), a magnetic field of 300 G was applied for 1100 h.

phenomenon was very similar to that shown in Fig. 3. However, in terms of time scales, this process was slower than the process shown in Fig. 3 due to the step-by-step change in the magnetic field.

The processes occurring while the magnetic field was slowly switched on and off, shown in Figs. 5 and 6, were analyzed by using Φ_6 and Φ_2, as shown in Fig. 7. At 300 G in Fig. 7(a), there was a small but abrupt change in the system, although this change is difficult to detect visually; however, the system soon returned to normal. This change may have been induced by the change in the director drift due to the changing magnetic field. However, as director drift stabilized, the stable structure returned. Φ_2 increased very smoothly approaching a limiting value. The increase seemed to be limited by the collapse of the long length structure. Finally, it reached a value close to zero.

The processes that occurred when the magnetic field was slowly switched off in Fig. 7(b) were very similar to the changes of Φ_6 and Φ_2, as shown in Fig. 4(a). There was no relaxation of the collapsed structure, and it extended suddenly at 140 G as shown in Fig. 3. It soon returned to a structure similar to that before the magnetic field was applied. Φ_2 maintained a value close to zero throughout the process. The turn-on and turn-off processes demonstrated that slightly different field strengths corresponded to the same stages of the change. It seems that there is some factor stabilizing the structure for both long and short distances between droplets.

The density of the droplets was found to be slightly dependent on the distance from the center. In the central area the density was higher than at the boundary. The ratio of the density variation was larger in the HL than in the dense HLL. However, tangential anisotropies in the density were not found. The density variation together with defects may deter the sharp peaks to be appeared in pair-correlation functions.

C. Discussion

The magnetic field applied normal to the LC layer did not seem to change the distance between droplets in the HL. Because the LC layer is thick, the deformation along the planar direction is very small and its effect may be negligible. The increase in temperature does not produce a clear change in the HL in the nematic LC phase in our system. However, the HL was completely disrupted at the nematic-isotropic phase transition temperature. This result is a little different from that discussed in Ref. [9]. The much larger droplet size (a diameter of about 20 μm) in this experiment may have weakened the thermal influence with increasing temperature compared to the previous experimental results (corresponding to droplets with a diameter of approximately 1 μm).

We applied a magnetic field of several hundred gauss. The magnetic coherence length $d_{\mathrm{M}} = \sqrt{K/\Delta\chi H^2}$, which is the transient length by the magnetic field, corresponded to approximately 70 μm with a magnetic field of 300 G [23]. The extrapolation length $d_{\mathrm{e}} = K/W$ of the free surface in 5CB was approximately 2 μm. K is the elastic constant and is close to the average of the splay and bend elastic constants (6.3 pN) [24]. W is the anchoring strength at the free surface of 5CB (10^{-5} J/m^2) [25]. Within the range of magnetic strengths used, the director at the interface rarely deviated from a vertical orientation. Because the droplet size was approximately 20 μm and most of the droplet was immersed in LC, the director around the droplet must be deformed by the magnetic field [7]. Without an applied magnetic field, a LC point defect is necessarily located directly below each droplet for thick LC layers. With an applied magnetic field, the point defect should move away from below the center of the droplet and induce a dipole-dipolelike interaction between droplets. Consequently, the CLA and a very closely packed HLL appear to have been realized.

The HL before the magnetic field was applied was a real two-dimensional hexagonal structure without anisotropy. However, the corresponding Φ_6 was approximately 0.4, and the structure was not quite a perfect HL. When the magnetic field was applied, the distance between droplets decreased, and neighboring droplets became closer. The Φ_6 increased to almost 0.7. In both cases, the distance between droplets varied with direction. In the case of HL, the variation of distance seemed to be very position dependent. It seems that there is no clear rule for this variation. The equilibrium distance was very sensitive and varied with parameters such as the droplet size and external influences. However, in the case of dense HLLs, the variation had a clear orientation dependency. When the average distance between nearest two points were considered, the distance between droplets perpendicular to the magnetic field was 10% longer than other orientations. This is very similar to the result found in a previous study [8]. However, in that case, there was no effective tool for inducing the anisotropy. A two-dimensional colloidal crystal constructed by a dipole-dipolelike interaction in the bulk LC showed that the lattice constant along the rubbing direction is slightly shorter than the lattice constant along the tilted direction [4]. In spite of the difference in values, the tendency of the structural arrangement and the anisotropic ratio of distances indicate that the magnetic field induced a dipole-dipolelike interaction.

The transition between the relatively well-ordered structures shown in the above processes included a random distribution, and we assessed this process in light of the well-known two-dimensional phase transition of the KTHNY theory. In the processes shown in Figs. 1 and 3, the initial and final structures indicated a power lawlike decay of $g(r)$ and $g_{\mathrm{B}}(r)$ with distance. Both exponents were much larger than the values predicted by the KTHNY theory for our experimental range. In the intermediate stage, the envelopes of both $g(r)$ and $g_{\mathrm{B}}(r)$ showed an exponential decay with distance. The transition from power law decay to exponential decay was not well defined. In other words, there was a smooth change from one to the other. In the HLL with short lattice spacing, the decay of both $g(r)$ and $g_{\mathrm{B}}(r)$ obeyed a power lawlike. The change to this phase also has a rather large exponent compared to that predicted by the KTHNY theory. The transition process induced by the magnetic field seems to deviate considerably from the KTHNY theory. The deviation may be due to the several aspects such as the variation of the droplet size, varying distribution for the localized aggregation of droplets, and insufficient droplets number to lessen the statistical variation.

IV. CONCLUSIONS

We observed the structural change of glycerol droplets realized on a LC surface due to a planar magnetic field. The HL was reduced to a HLL with shorter lattice spacings. The dense structure shows anisotropy in lattice constants, and it seems that this structure is formed due to the dipole-dipolelike interaction induced by the magnetic field. The transition process was influenced by the manner in which the magnetic field was applied. With a sufficiently high magnetic field, the transition proceeded through a random structural arrangement and then CLA. However, with a step-by-step increase in magnetic field strength, the change began in a localized region and gradually extended throughout the entire region.

The relaxation after the magnetic field was switched off began at the outside and extended into the central regions. No tendency to form a chainlike arrangement was observed during the relaxation process. The processes observed during the switching on and off demonstrated a hysteresis with the magnetic field. Therefore, it seems that these structures are stable over some ranges of magnetic field strength.

ACKNOWLEDGMENT

This study was financially supported by the 2010 research fund of Chungnam National University.

[1] P. Poulin, H. Stark, T. C. Lubensky, and D. A. Weitz, Science **275**, 1770 (1997).
[2] T. C. Lubensky, D. Pettey, N. Currier, and H. Stark, Phys. Rev. E **57**, 610 (1998).
[3] J. C. Loudet, P. Barois, and P. Poulin, Nature (London) **407**, 611 (2000).
[4] I. Musevic, M. Skarabot, U. Tkalec, M. Ravnik, and S. Zumer, Science **313**, 954 (2006).
[5] C. P. Lapointe, T. G. Mason, and I. I. Smalyukh, Science **326**, 1083 (2009).
[6] V. G. Nazarenko, A. B. Nych, and B. I. Lev, Phys. Rev. Lett. **87**, 075504 (2001).
[7] I. I. Smalyukh, S. Chernyshuk, B. I. Lev, A. B. Nych, U. Ognysta, V. G. Nazarenko, and O. D. Lavrentovich, Phys. Rev. Lett. **93**, 117801 (2004).
[8] A. B. Nych, U. M. Ognysta, V. M. Pergamenshchik, B. I. Lev, V. G. Nazarenko, I. Musevic, M. Skarabot, and O. D. Lavrentovich, Phys. Rev. Lett. **98**, 057801 (2007).
[9] A. Brodin, A. Nych, U. Ognysta, B. I. Lev, V. Nazarenko, M. Skarabot, and I. Musevic, Condens. Matter Phys. **13**, 33601 (2010).
[10] B. I. Lev, A. Nych, U. Ognysta, D. Reznikov, S. Chernyshuk, and V. Nazarenko, JETP Lett. **75**, 322 (2002).
[11] K. Chen, T. Kaplan, and M. Mostoller, Phys. Rev. Lett. **74**, 4019 (1995).
[12] A. H. Marcus and S. A. Rice, Phys. Rev. Lett. **77**, 2577 (1996).
[13] A. H. Marcus and S. A. Rice, Phys. Rev. E **55**, 637 (1997).
[14] T. Terao and T. Nakayama, Phys. Rev. E **60**, 7157 (1999).
[15] B. J. Lin and L. J. Chen, J. Chem. Phys. **126**, 034706 (2007).
[16] Y. Han, N. Y. Ha, A. M. Alsayed, and A. G. Yodh, Phys. Rev. E **77**, 041406 (2008).
[17] U. Gasser, C. Eisenmann, G. Maret, and P. Keim, Chem. Phys. Chem. **11**, 963 (2010).
[18] M. A. Gharbi, M. Nobili, M. In, G. Prevot, P. Galatola, J. B. Fournier, and C. Blanc, Soft Matt. **7**, 1467 (2011).
[19] T. Yamamoto, J. Yamamoto, B. I. Lev, and H. Yokoyama, Appl. Phys. Lett. **81**, 2187 (2002).
[20] T. Yamamoto and M. Yoshida, Appl. Phys. Express **2**, 101501 (2009).
[21] B. I. Lev, S. B. Chernyshuk, T. Yamamoto, J. Yamamoto, and H. Yokoyama, Phys. Rev. E **78**, 020701(R) (2008).
[22] S. B. Chernyshuk, O. M. Tovkach, and B. I. Lev, Phys. Rev. E **85**, 011706 (2012).
[23] D. S. Wiersma, A. Muzzi, M. Colocci, and R. Righini, Phys. Rev. E **62**, 6681 (2000).
[24] N. V. Madhusudana and R. Pratibha, Mol. Cryst. Liq. Cryst. **89**, 249 (1982).
[25] O. D. Lavrentovich and V. M. Pergamenshchik, Phys. Rev. Lett. **73**, 979 (1994).